



Article

Probing Contact Electrification between Gas and Solid Surface

Linlin Sun^{1,2}, Ziming Wang¹, Chengyu Li¹ , Wei Tang^{1,3,4,*} and Zhonglin Wang^{1,3,5,*}

¹ CAS Center for Excellence in Nanoscience, Beijing Institute of Nanoenergy and Nanosystems, Chinese Academy of Sciences, Beijing 101400, China

² College of Mechanical and Electronic Engineering, Shandong Agricultural University, Taian 271000, China

³ School of Nanoscience and Technology, University of Chinese Academy of Sciences, Beijing 100049, China

⁴ Institute of Applied Nanotechnology, Jiaxing 314031, China

⁵ School of Materials Science and Engineering, Georgia Institute of Technology, Atlanta, GA 30332, USA

* Correspondence: tangwei@binn.cas.cn (W.T.); zhong.wang@mse.gatech.edu (Z.W.)

Abstract: Contact electrification exists everywhere and between every phase of matter. However, its mechanism still remains to be studied. The recent triboelectric nanogenerator serves as a probe and provides some new clues about the mechanism present in solid–solid, solid–liquid, and liquid–liquid contact electrification. The gas–solid model still remains to be exploited. Here, we investigated the contact electrification between gases and solids based on the single-electrode triboelectric nanogenerator. Our work shows that the amount of transferred charges between gas and solid particles increases with surface area, movement distance, and initial charges of particle increase. Furthermore, we find that the initial charges on the particle surface can attract more polar molecules and enhance gas collisions. Since ions in gas–solid contact are rare, we speculate that gas–solid contact electrification is mainly based on electron transfer. Further, we propose a theoretical model of gas–solid contact electrification involving the gas collision model and initial charges of the particle. Our study may have great significance to the gas–solid interface chemistry.

Keywords: gas–solid interface; contact electrification; triboelectric nanogenerator; gas collision



Citation: Sun, L.; Wang, Z.; Li, C.; Tang, W.; Wang, Z. Probing Contact Electrification between Gas and Solid Surface. *Nanoenergy Adv.* **2023**, *3*, 1–11. <https://doi.org/10.3390/nanoenergyadv3010001>

Academic Editors: Federico Rosei and Ya Yang

Received: 17 October 2022

Revised: 23 December 2022

Accepted: 26 December 2022

Published: 2 January 2023



Copyright: © 2023 by the authors. Licensee MDPI, Basel, Switzerland. This article is an open access article distributed under the terms and conditions of the Creative Commons Attribution (CC BY) license (<https://creativecommons.org/licenses/by/4.0/>).

1. Introduction

Contact electrification (CE) is universal and has been known for over 2600 years. However, its mechanism still remains debated. Many researchers have focused on the solid–solid CE. Several mechanisms are proposed [1–3], such as the emergence of a triboelectric nanogenerator [4–6], with new clues being discovered [7–9]. Subsequently, liquid–solid and liquid–liquid CE models are also investigated [10–14], which shed some light on fundamental insights into the CE mechanism. However, as another phase, gas exists everywhere, but gas–solid CE is rarely reported. So far, sensing systems involving gas have been researched based on TENG [15–19]. It is worth noting that the gas–solid interacted power generation is proposed by exploiting the gas–solid interface to harness triboelectricity [20]. In addition, it has been recently proved that gases (such as O₂, N₂, O₃, H₂, and so forth) have a significant effect on the solid–solid contact electrification and solid–liquid contact electrification [21–25]. However, compared to solid–solid contact electrification and solid–liquid contact electrification, the mechanism of gas–solid contact electrification has not yet been researched systematically.

Here, we investigate the mechanism of the electrification between gases and solids. Charge transferring is probed based on the single-electrode TENG. The influence of surface area, movement distance, and the initial charges of solid on gas–solid CE are examined. Moreover, we analyze the contribution of the initial charges of the solid to the gas adsorption law. Finally, a model of the gas–solid contact electrification and gas collision model involving the initial charges of the solid is proposed, providing a distinct mechanism from the general understanding of classical gas–solid interface chemistry.

2. Materials and Methods

Electrical Measurement: The measuring device was designed based on the single-electrode TENG. The induction electrode, made of copper foil (35 μm thick), was designed to be hollow cylinders. To completely measure the charge on the surface of the polymer, the diameter and height of the induction electrode were 8 cm and 10 cm, respectively. All charges on the induction electrode derived from the charged solid were measured by connecting the electrode with a Keithley 6517b electrometer. All tests in the experiment were repeated more than 20 times, and the mean value was used for the results in the figure.

Simulation method: The fluid dynamics simulation between the polymer (PTFE) and gas was completed by FLUENT. The simulation is carried out under ideal gas conditions. The turbulent model is SST k- ω . The pressure of the inlet and outlet was set to 101.325 kPa. The density of PTFE was set to 2.2 g/cm^3 . PTFE was in free fall during the simulation, and the fall time was set to 200 ms. The pressure and velocity of the flow field were detected during the free fall of PTFE.

3. Results and Discussion

Figure 1a(i) shows a dynamic testing process of gas–solid contact electrification. The number of transferred charges (ΔQ) was measured based on the single-electrode triboelectric nanogenerator, with the induction electrodes installed in a Faraday Cage, which shields the interference of the external electric field. The induction electrode is made of copper foil (35 μm thick and 10 cm width), with a size larger than solid particles. As illustrated in Figure 1a(ii), when the charged solid passes through the induction electrode, electrons are exchanged between the electrode and the ground due to electrostatic induction. During the experiments, the solid free falls from the top to the bottom of the Faraday cage, successively passing through the top and bottom induction electrodes, as shown in Figure S1. The charge on the solid surface is measured through the charging and discharging of the capacitance inside the electrometer. When the solid enters the top electrode, the capacitance of the top electrometer begins to charge. As the solid continues to fall, the solid passes through the top electrode and enters the bottom electrode. At this time, the discharge of the top electrometer capacitor is not finished, while the bottom electrometer capacitor begins to charge. Therefore, the two charge curves partially overlap. Corresponding charge testing curves are plotted in Figure 1b. The time interval of the two peaks was about 0.13 s, which correlated well with the particle's practical movement. The measured transfer charges of the top electrode were defined as Q_{top} , and that of the bottom electrode was defined as Q_{bottom} . Therefore, the number of transferred charges (ΔQ) between gas and solid during the free fall can be obtained by the formula $\Delta Q = Q_{bottom} - Q_{top}$.

Figure 1c shows the fluid dynamics simulation. It indicates that the bottom surface of the solid is in a compression state, which means that collisions with gas molecules mainly occur in this area. Figure S2 shows that as the speed increases, the pressure increases, suggesting that more collisions happen. Subsequently, we examined the gas molecule distribution under different surface areas and speeds, as shown in Figure 1d. The arrows in Figure 1d indicate the velocity direction of the airflow around the fall path. PTFE ball colors in Figure 1d represent the surface pressure between the solid and gas. We found that gas molecules around the solid take part in solid–gas collisions due to the compressed region generated at the bottom of the solid. We also carried out aerodynamic simulation analysis for the case of other surface areas, as shown in Figure S3a,b, and the results were consistent with Figure 1c,d. Figure S3c shows the change of gas pressure around the solid during movement. The negative pressure around the bottom of the solid is created due to the motion of the solid, while the gas pressure around the solid is not affected. In consequence, the pressure difference is formed around the solid and drives more molecules to collide with the solid. Consequently, we speculate that the ΔQ of gas–solid contact electrification is affected by the surface area and speed of the solid.

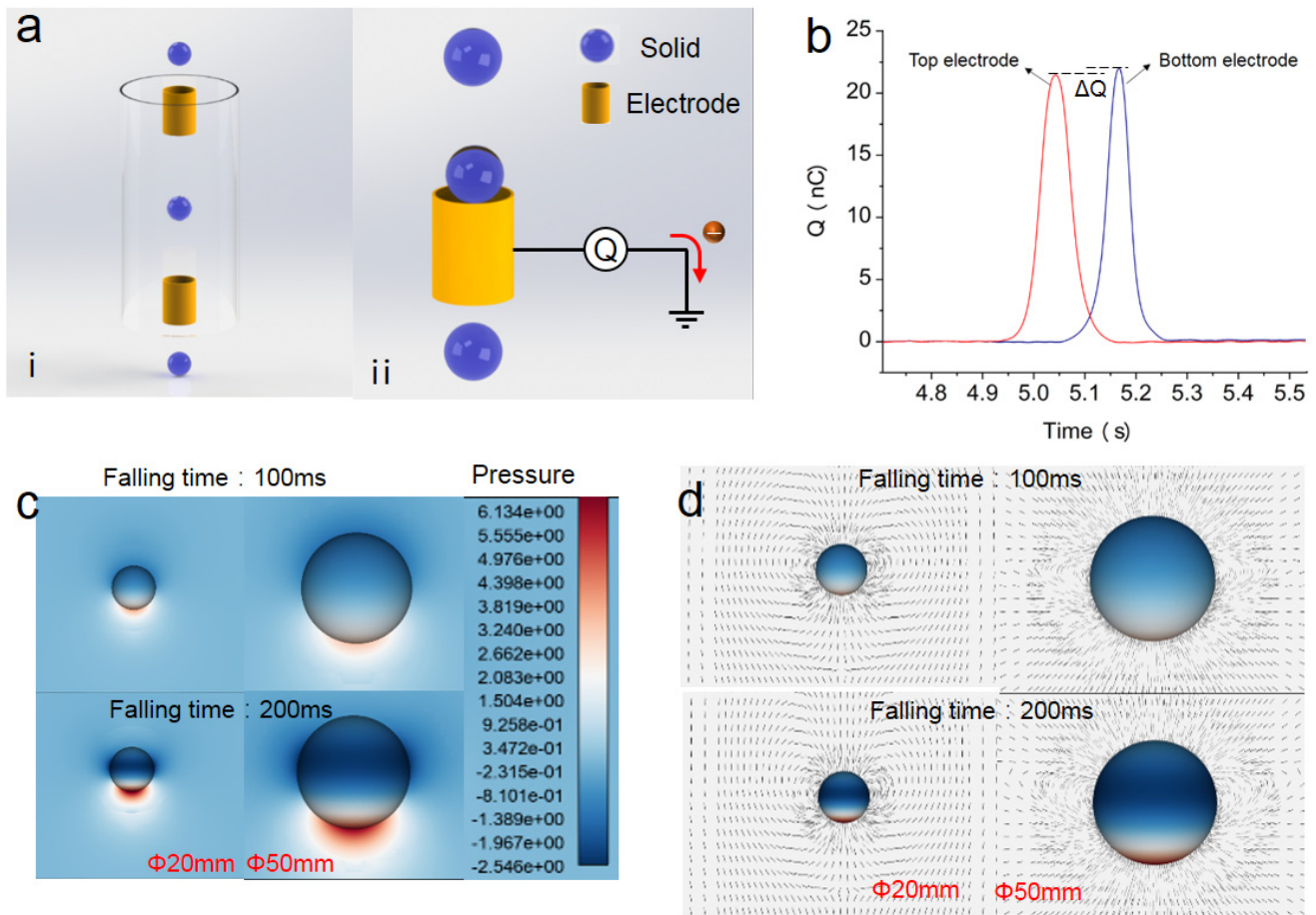


Figure 1. Experimental principle and fluid dynamics simulation. (a) The testing principle of gas–solid contact electrification. The device is designed based on single-electrode TENG. The solid is thrown from the top of the container in free fall, passing through the top and bottom induction electrodes, respectively. (b) The testing result of the top and bottom electrodes. (c) The change of the pressure around the solid. (d) The effect of surface area and speed on the distribution of gas molecules.

Afterward, we systematically examined gas–solid contact electrification. Five kinds of polymer particles of polycarbonate (PC), polyamide (PA), polytetrafluoroethylene (PTFE), polyoxymethylene (POM), polypropylene (PP) with different diameters, ranging from 20 to 50 mm were selected. The gas pressure during the test was set to 101.325 kPa. They free fall from the same height above the top induction electrode, as shown in Figure 2a. Figure 2b shows the testing results of PC particles. It indicates that the ΔQ increases as the diameter increases, meaning that the larger surface area of the particle will induce more transferred charge. This corresponds well with the above simulations in Figure 1c. As the diameter increases, the collision probability and times between the particles and gas molecules increase. Subsequently, other materials were tested under the same conditions, and the results are plotted in Figure 2c–f. Those results lead to the same conclusion. It is worth noting that the gas–solid contact electrification is related to the electron-withdrawing ability of the solid. Meanwhile, the electron-withdrawing ability depends on the surface functional groups of the polymer. Therefore, the gas–solid contact electrification properties can be influenced by the physical and chemical properties of the solid materials.

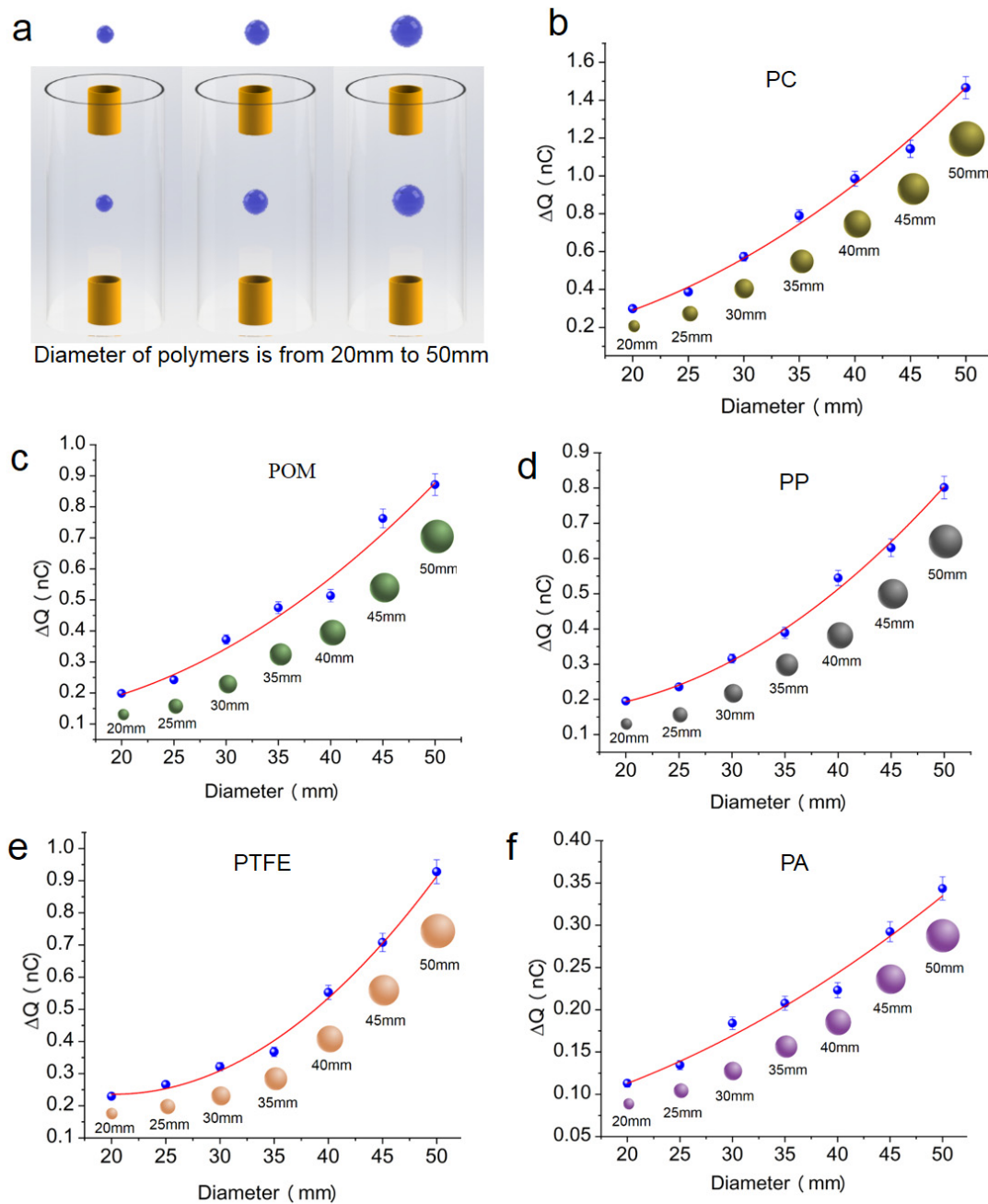


Figure 2. Effects of surface area on gas–solid contact electrification. (a) The testing principle of gas–solid contact electrification under different contact areas. (b–f) The relationship between the transferred charge and the contact area in the process of gas–PC, gas–POM, gas–PP, gas–PTFE, and gas–PA contact electrification.

Moreover, the additional experiment was performed in a clean room, and testing results are illustrated in Figure 3a. The particle concentrations inside the clean room were class 10,000 and outside the clean room were class 1,000,000. The charge transferring during gas–solid electrification in the clean room was close to that in normal circumstances. The effect of floating particles in the air is small, which might be attributed to the number of collisions with floating particles being much less than with gas molecules.

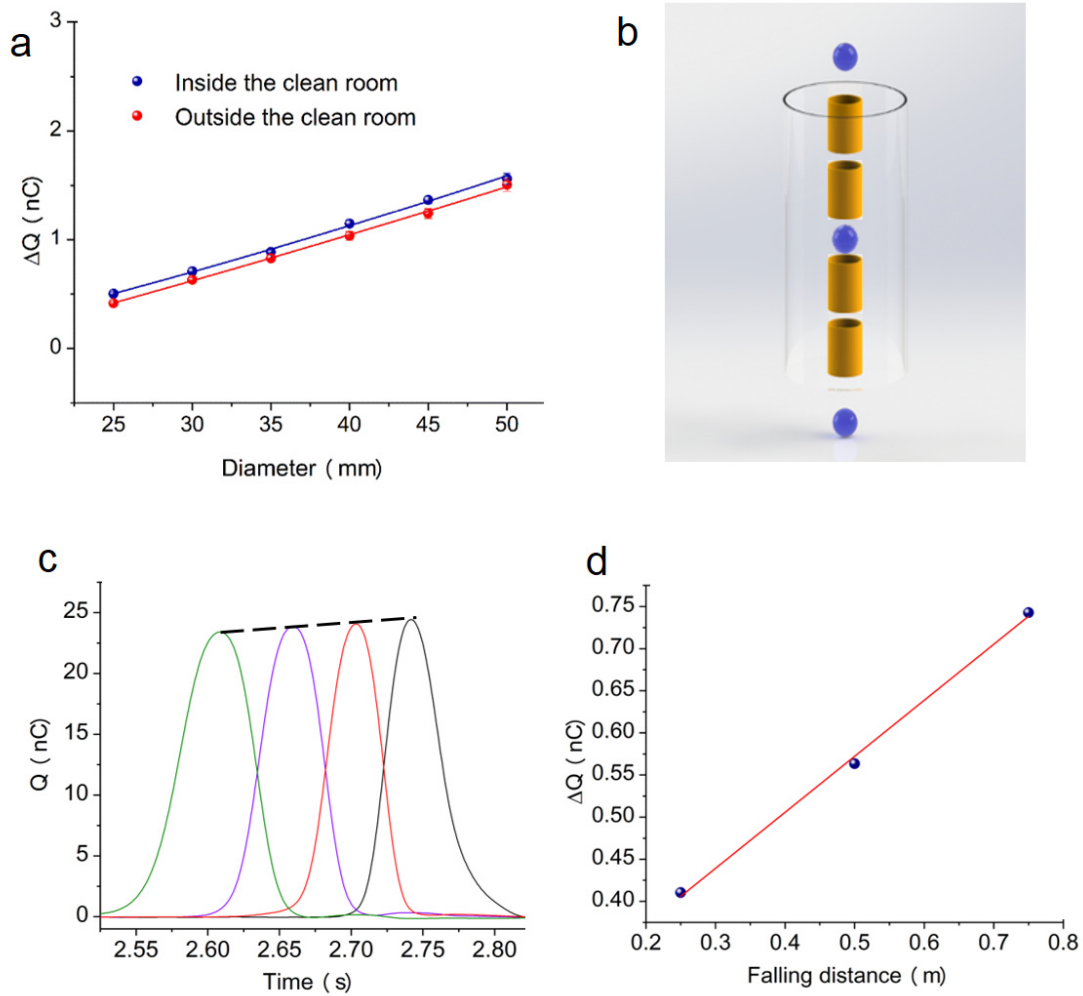


Figure 3. Effects of floating particles in the air and falling distance on gas–solid contact electrification. (a) The result of gas–solid electrification inside and outside the clean room. (b) The testing principle of different falling distances. (c) The output of the electrometer under different falling distances. (d) The relationship between the transferred charge and the falling distance.

Additionally, we investigated the effect of falling distance (0.25 m, 0.5 m, 0.75 m) on the gas–solid contact electrification, as shown in Figure 3b. Figure 3c–d show that as the falling distance increases, the transferred charges increase linearly. Accordingly, we speculate that the transferred charges are proportional to the collisions between the particle and gas molecules, which are determined by the gas molecule quantity.

Considering that the density of gas molecules is n , falling distance is h , diameter of the particle is D , and assuming that the solid particle collides with all gas molecules in its falling pathway, the derivation is modeled based on the mean free path of gas molecules. When the number density of the gas molecules is n , the number of collisions during the particle falling can be expressed as (detailed formula derivation can be found in supporting information Note 1):

$$N = \frac{1}{4}nh\pi D^2 \tag{1}$$

There is a charge-transferring coefficient of η caused by contact electrification. Therefore, the ΔQ can be expressed by:

$$\Delta Q = \frac{1}{4}\eta nh\pi D^2 \tag{2}$$

In addition, we can obtain the η from the diameter and falling height test, which is about 2.3×10^{-23} nC. Subsequently, the η of other materials were calculated, and results are listed in Supplementary Materials Table S1. Divided by the charge amount of one single electron, we obtain another coefficient of 1.44×10^{-13} , implying the electron transferring probability during one collision.

Additionally, it is worth noting that in the experiments, the ΔQ will be influenced by the initial charges on the polymer surface. Testing results on PC particles are shown in Figure 4a. It can be seen that ΔQ increases as the initial charges increase. The same results for other materials can be seen in Figure 4b–e. It shows that the initial charges on the polymer surface act as an “amplifier” in the process of gas–solid contact electrification, which can effectively improve the solid’s electrification performance. It is found that the explored range of initial charge density varies with different materials. Due to the different electron-withdrawing abilities of materials, it is difficult to get some materials highly initially charged, thus, leading to differences in the range of initial charge densities. We speculate that the initial charges attract more gas molecules around. Therefore, we make a modification to Equation (2) as follows:

$$\Delta Q = \frac{1}{4} \eta n (1 + \alpha q) h \pi D^2 \quad (3)$$

where αq represents the modification in the gas number density caused by the charges. Additionally, we obtain a differential equation:

$$dq = \frac{\eta n \pi D^2}{4} (1 + \alpha q) dh \quad (4)$$

After replacing $\eta n \pi D^2 / 4$ with A , it can be expressed as:

$$\frac{dq}{dh} = A + A \alpha q \quad (5)$$

Therefore, q can be solved as:

$$q = q_0 \left[\left(1 + \frac{1}{\alpha q_0} \right) e^{A \alpha h} - \frac{1}{\alpha q_0} \right] \quad (6)$$

Furthermore, ΔQ can be calculated as:

$$\Delta Q = q_0 \left(1 + \frac{1}{\alpha q_0} \right) (e^{A \alpha h} - 1) \quad (7)$$

It is worth noting that if we assume a small modification in the gas number density caused by the charges, i.e., αq and αq_0 are small, Equation (7) can be turned into:

$$\Delta Q = Ah \quad (8)$$

which corresponds well with Equation (1).

Furthermore, we compare the effect of positive and negative initial charges on gas–solid contact electrification, as shown in Figure 4f. No obvious difference was found.

To further verify our above hypothesis, we repeated the gas–solid contact electrification under a non-polar-gas-rich and polar-gas-rich atmosphere. Pure nitrogen (N_2) and oxygen (O_2) were chosen as the non-polar gas sources and continuously injected into the container, respectively, during the experiment. Testing results in O_2 -rich and N_2 -rich conditions are plotted in Figure 5a–f, showing that the ΔQ increases more significantly in the air than in those two conditions as the initial density increases.

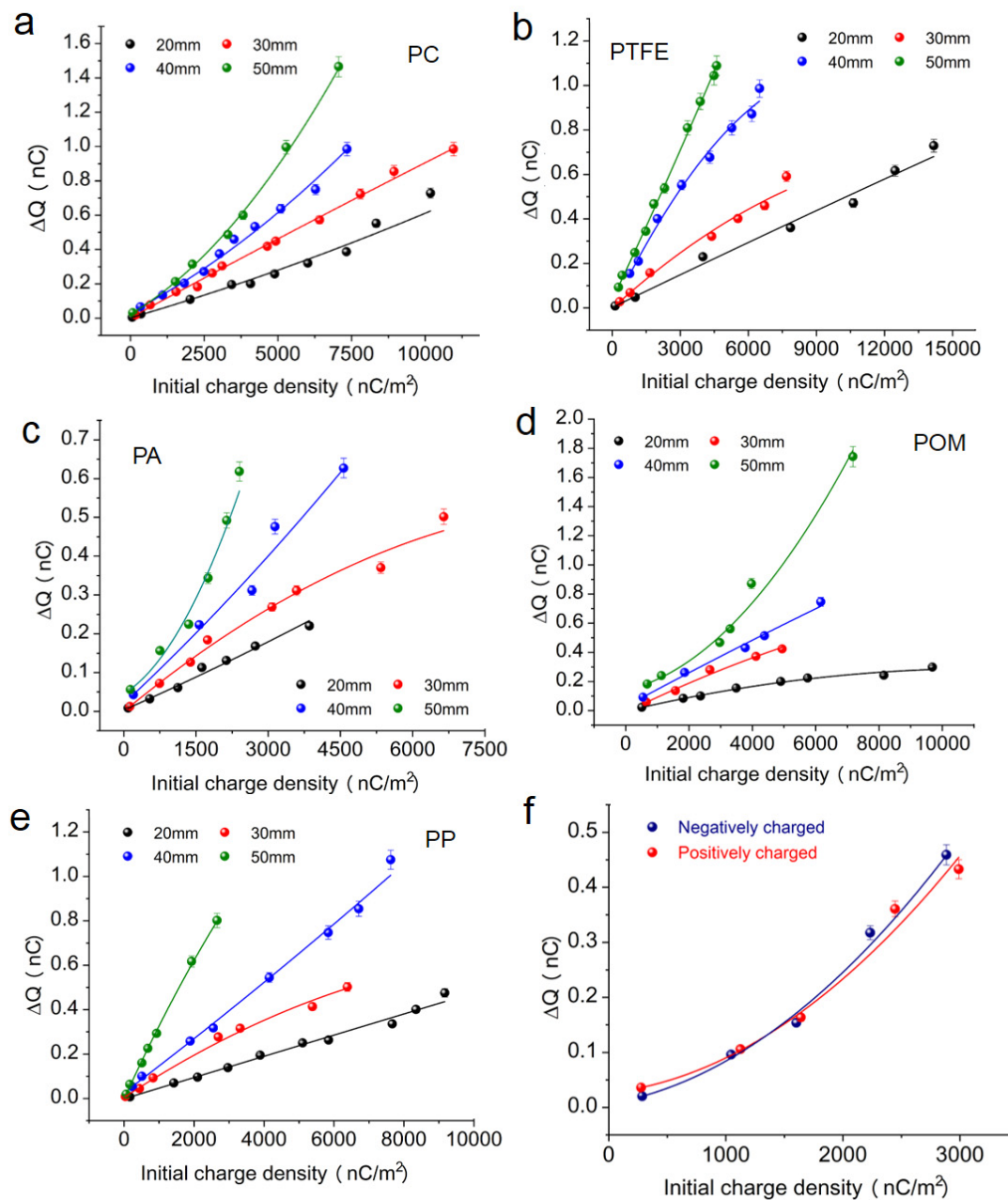


Figure 4. Effects of initial charge on polymer surface at gas–solid contact electrification. (a–e) The relationship between the transferred charge and initial charge of the polymer surface in the process of gas–PC, gas–PTFE, gas–PA, gas–POM, and gas–PP contact electrification. (f) The effect of initial charge polarity on electron transfer.

On the contrary, we chose water gas molecules (H_2O) to create a polar-gas-rich environment. The experiment was operated at the humidity of 20%, 30%, 40%, and 60%. Testing results are illustrated in Figure 5g–i. Apparently, the ΔQ increases as the initial charge increases, and the enhancement is promoted when the humidity gets larger. That verified our hypothesis that the initial charges on the particle will attract polar gas molecules and thus enhance the gas–solid collisions and charge transferring. However, as the humidity continues to increase to 60%, the ΔQ decreases, which means that higher humidity can reduce the charge transfer during gas and solid contact electrification. It is worth noting that the previous research obtained the same result [26]. We speculate that contact electrification mainly occurred between gas and solid under low humidity conditions, while contact

electrification between gas and solid would be suppressed at high humidity. Additionally, we tried another polar gas molecule, i.e., ethanol. The testing result is plotted in Figure 6a. An apparent enhancement was found with ethanol filled in, consistent with our results obtained in the H₂O-rich condition. Therefore, we demonstrated that gas–solid contact electrification can be enhanced during polar-gas-molecule conditions.

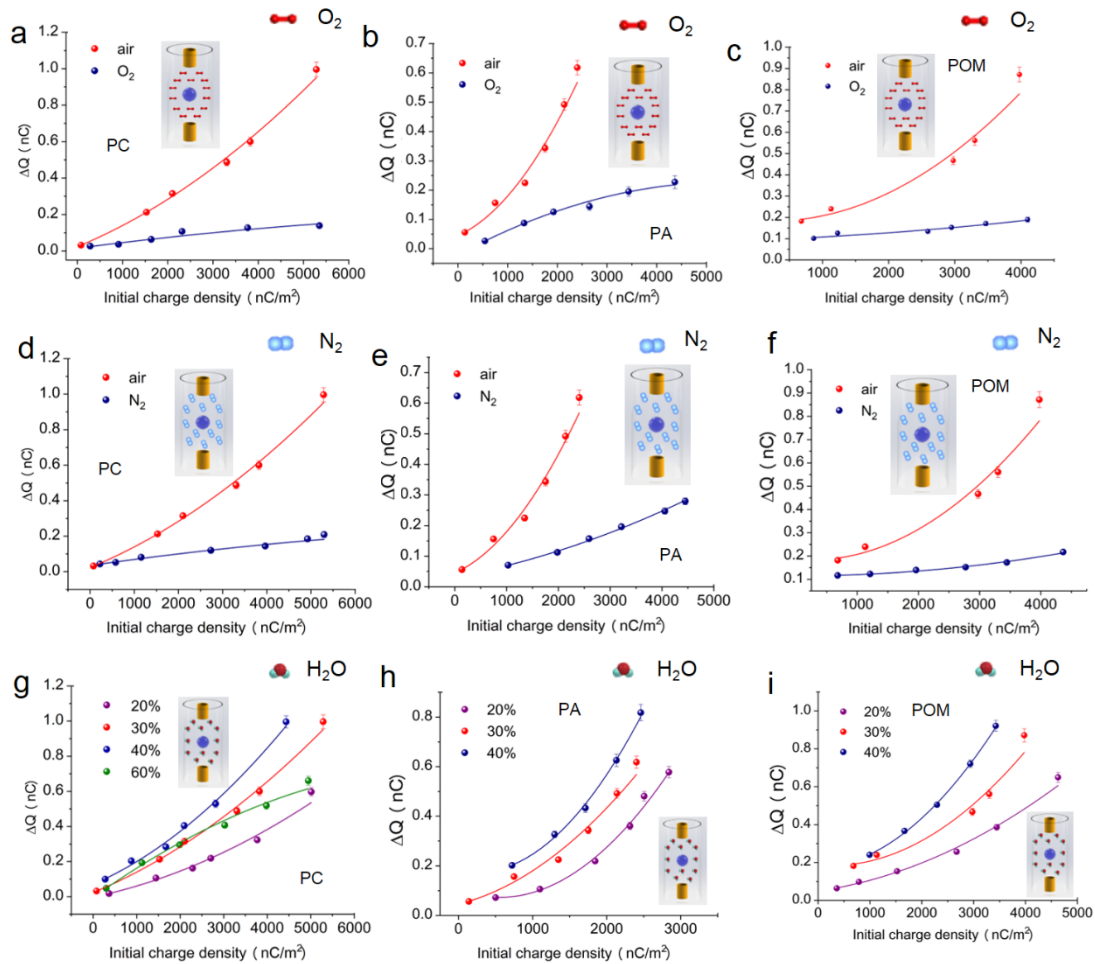


Figure 5. The difference between gas–polymer contact electrification in the non-polar-gas-rich atmosphere and polar-gas-rich atmosphere. (a–c) The effect of the non-polar-gas-rich atmosphere (O₂) on gas–PC, gas–PA, and gas–POM contact electrification. (d–f) The effect of the non-polar-gas-rich atmosphere (N₂) on gas–PC, gas–PA, and gas–POM contact electrification. (g–i) The effect of the polar-gas-rich atmosphere (H₂O) on gas–PC, gas–PA, and gas–POM contact electrification. The concentration is 20%, 30%, 40%, 60%.

In addition, owing to bare ions existing in gas/solid contact, we can speculate that the solid/gas contact electrification is mainly dominated by electron transfer. The specific theory model is shown in Figure 6b. When the state of initial charges on the polymer surface is neutral (Figure 6b (i)), the gas collision of the polymer follows the traditional gas collision law. The number of molecules colliding with the solid is n_1 , and the amount of transferred charges between the gas and solid is ΔQ_1 . When the initial charges exist on the polymer surface, the solid begins to attract more polar molecules toward the surface in a targeted manner (Figure 6b (ii)). The amount of molecules (n_2) colliding with the solid thus increases. The amount of transferred charges between gas and polymer is ΔQ_2 . Figure 6b (iii) shows that the initial charges on the polymer surface continue to increase, which means that the polymer can attract polar molecules from farther away. The amount of molecules (n_3) colliding with polymers continues to increase. The amount of transferred charges

between gas and polymer is ΔQ_3 . According to the above analysis, we can conclude that $n_1 < n_2 < n_3$ and $\Delta Q_1 < \Delta Q_2 < \Delta Q_3$.

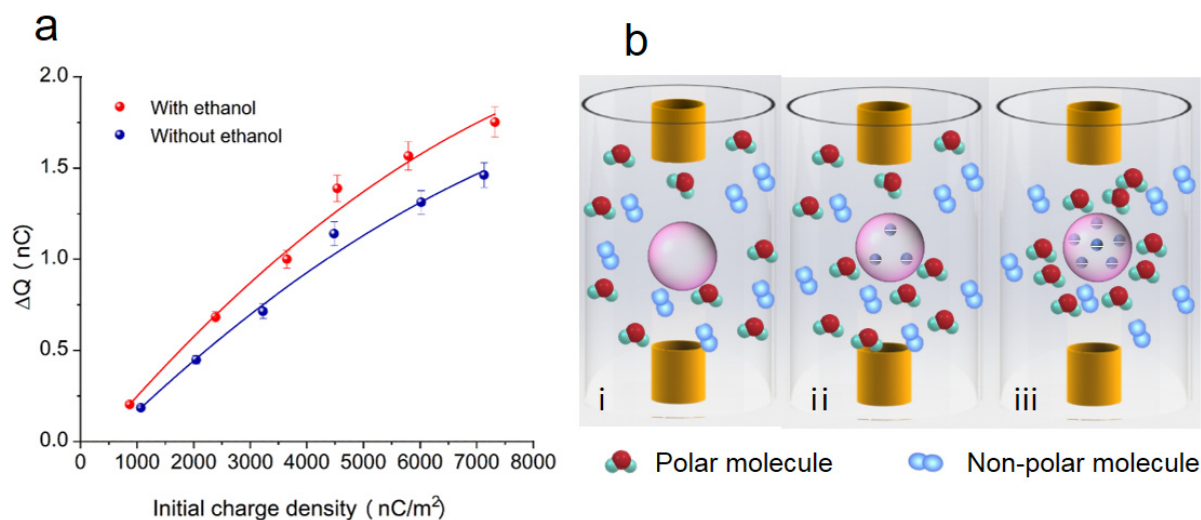


Figure 6. The influence of initial charges and atmosphere on gas-polymer contact electrification. (a) The effect of the polar-gas-rich atmosphere (ethanol) on contact electrification. (b) The gas collision model involving the initial charge on the solid surface.

4. Conclusions

In this work, we designed a non-contact measurement approach based on the single-electrode triboelectric nanogenerator for studying gas–solid CE, which can obtain direct and reliable results. We found that the gas–solid CE will be determined by the solid surface area, movement distance, initial charge density, and gas conditions. As the solid area and movement distance become larger, the gas–solid CE will be enhanced. Moreover, the initial charge density of the solid can also enhance the gas–solid CE due to the surface charges attracting polar gas molecules, leading to more colliding between the solid and gas molecules. The hypothesis was verified by the experiments performed under polar and non-polar gas conditions. Furthermore, theory models of gas–solid CE based on the ideal gas approximation are discussed. Our work may have a great impact on the further investigation of gas–solid and gas–liquid contact electrification. Furthermore, this work shows the possibility of adjusting the interfacial charge between the gas and solid, showing potential applications in the gas–solid interface chemistry.

Supplementary Materials: The following supporting information can be downloaded at: <https://www.mdpi.com/article/10.3390/nanoenergyadv3010001/s1>; Note 1: Formula derivation for the transferred charge amount during a solid particle falling. Table S1: The η of other materials. Figure S1: The movement process of the polymer. (a) The correspondence between output of electrometer and motion of polymer. (b) Snapshots showing the motion of the polymer. Figure S2: The relationship between pressure and velocity. Figure S3: Fluid dynamics simulation between gas and polymers. (a) The pressure between the gas and polymer surface changes with the contact area. (b) The influence of contact area and velocity on the distribution of gas molecules. (c) The changes of gas pressure around the polymer and the motion trends of gas molecules.

Author Contributions: Conceptualization, W.T. and Z.W. (Zhonglin Wang); methodology, L.S.; software, L.S. and Z.W. (Ziming Wang); validation, L.S. and C.L.; formal analysis, L.S.; investigation, L.S.; resources, Z.W. (Ziming Wang) and C.L.; data curation, L.S.; writing—original draft preparation, L.S., Z.W. (Ziming Wang), C.L., and W.T.; writing—review and editing, L.S., Z.W. (Ziming Wang), C.L., W.T., and Z.W. (Zhonglin Wang); visualization, L.S. and C.L.; supervision, W.T. and Z.W. (Zhonglin Wang); project administration, W.T.; funding acquisition, W.T. and Z.W. (Zhonglin Wang). All authors have read and agreed to the published version of the manuscript.

Funding: This research was funded by the National Key R&D Project by the Minister of Science and Technology (Grant No. 2016YFA0202704), National Natural Science Foundation of China (Grant Nos. 51432005 and 5151101243), Beijing Municipal Science and Technology Commission (Grant Nos. Z181100003818016, Z171100000317001, Z171100002017017, and Y3993113DF), China Postdoctoral Science Foundation (2019M660766), and Youth Innovation Promotion Association, CAS.

Data Availability Statement: Data are contained within the article and Supplementary Materials.

Conflicts of Interest: The authors declare no conflict of interest.

References

1. Lin, Z.; Xie, Y.; Yang, Y.; Wang, S.; Zhu, G.; Wang, Z.L. Enhanced Triboelectric Nanogenerators and Triboelectric Nano- sensor Using Chemically Modified TiO₂ Nanomaterials. *ACS Nano* **2013**, *7*, 4554–4560. [[CrossRef](#)] [[PubMed](#)]
2. Lee, J.; Cho, H.; Chun, J.; Kim, K.; Kim, S.; Ahn, C.; Kim, I.; Kim, J.; Kim, S.; Yang, C.; et al. Robust Nanogenerators Based on Graft Copolymers via Control of Dielectrics for Remarkable Output Power. *Sci. Adv.* **2017**, *3*, 1602902. [[CrossRef](#)] [[PubMed](#)]
3. Shin, S.; Bae, Y.; Moon, H.; Kim, J.; Choi, S.; Kim, Y.; Yoon, H.; Lee, M.; Nah, J. Formation of Triboelectric Series via Atomic-Level Surface Functionalization for Triboelectric Energy Harvesting. *ACS Nano* **2017**, *11*, 6131–6138. [[CrossRef](#)] [[PubMed](#)]
4. Fan, F.R.; Tian, Z.Q.; Wang, Z.L. Flexible Triboelectric Generator! *Nano Energy* **2012**, *1*, 328–334. [[CrossRef](#)]
5. Zhu, G.; Bai, P.; Chen, J.; Jing, Q.; Wang, Z.L. Triboelectric nanogenerators as a new energy technology: From fundamentals, devices, to applications. *Nano Energy* **2015**, *14*, 126–138. [[CrossRef](#)]
6. Wang, Z.L. Triboelectric Nanogenerators as New Energy Technology for Self-Powered Systems and as Active Mechanical and Chemical Sensors. *ACS Nano* **2013**, *7*, 9533–9557. [[CrossRef](#)]
7. Lin, S.; Xu, L.; Zhu, L.; Chen, X.; Wang, Z.L. Electron Transfer in Nanoscale Contact Electrification: Photon Excitation Effect. *Adv. Mater.* **2019**, *31*, 1901418. [[CrossRef](#)]
8. Zhang, Y.; Shao, T. Contact Electrification Between Polymers and Steel. *J. Electrostat.* **2013**, *71*, 862–866. [[CrossRef](#)]
9. Wu, J.; Wang, X.; Li, H.; Wang, F.; Hu, Y. First-Principles Investigations on the Contact Electrification Mechanism between Metal and Amorphous Polymers for Triboelectric Nanogenerators. *Nano Energy* **2019**, *63*, 103864. [[CrossRef](#)]
10. Shahzad, A.; Wijewardhana, K.R.; Song, J.K.J. Contact Electrification Efficiency Dependence on Surface Energy at the Water- Solid Interface. *Appl. Phys. Lett.* **2018**, *113*, 023901. [[CrossRef](#)]
11. Choi, D.; Lee, S.; Park, S.; Cho, H.; Hwang, W.; Kim, D. Energy Harvesting Model of Moving Water Inside a Tubular System and its Application of a Stick-Type Compact Triboelectric Nano- generator. *Nano Res.* **2015**, *8*, 2481–2491. [[CrossRef](#)]
12. Yin, J.; Zhang, Z.; Li, X.; Zhou, J.; Guo, W. Harvesting Energy from Water Flow over Graphene. *Nano Lett.* **2011**, *12*, 1736–1741. [[CrossRef](#)] [[PubMed](#)]
13. Jeon, S.; Seol, M.; Kim, D.; Park, S.; Choi, Y. Self-Powered ion Concentration Sensor with Triboelectricity from Liquid-Solid Contact Electrification. *Adv. Electron. Mater.* **2016**, *2*, 160006. [[CrossRef](#)]
14. Kwak, S.; Lin, S.; Lee, J.; Ryu, H.; Kim, T.; Zhong, H.; Chen, H.; Kim, S. Triboelectrification-Induced Large Electric Power Generation from a Single Moving Droplet on Graphene/Polytetra- fluoroethylene. *ACS Nano* **2016**, *10*, 7297–7302. [[CrossRef](#)]
15. Wang, Y.; Liu, D.; Hu, Z.; Chen, T.; Zhang, Z.; Wang, H.; Du, T.; Zhang, S.L.; Zhao, Z.; Zhou, T.; et al. A Triboelectric- Nanogenerator-Based Gas-Solid Two-Phase Flow Sensor for Pneumatic Conveying System Detecting. *Adv. Mater. Technol.* **2021**, *6*, 2001270. [[CrossRef](#)]
16. Wang, D.; Zhang, D.; Yang, Y.; Mi, Q.; Zhang, J.; Yu, L. Multifunctional Latex/Polytetrafluoroethylene-Based Triboelectric Nanogenerator for Self-Powered Organ-like MXene/Metal–Organic Framework-Derived CuO Nanohybrid Ammonia Sensor. *ACS Nano* **2021**, *15*, 2911–2919. [[CrossRef](#)] [[PubMed](#)]
17. Zhang, D.; Wang, D.; Xu, Z.; Zhang, X.; Yang, Y.; Guo, J.; Zhang, B.; Zhao, W. Diversiform sensors and sensing systems driven by triboelectric and piezoelectric nanogenerators. *Coord. Chem. Rev.* **2021**, *427*, 213597. [[CrossRef](#)]
18. Zhang, D.; Yang, Z.; Li, P.; Pang, M.; Xue, Q. Flexible self-powered high-performance ammonia sensor based on Audecorated MoSe₂ nanoflowers driven by single layer MoS₂-flake piezoelectric nanogenerator. *Nano Energy* **2019**, *65*, 103974. [[CrossRef](#)]
19. Zhang, D.; Xu, Z.; Yang, Z.; Song, X. High performance flexible self-powered tin disulfide nanoflowers/reduced graphene oxide nanohybrid-based humidity sensor driven by triboelectric nanogenerator. *Nano Energy* **2020**, *67*, 104251. [[CrossRef](#)]
20. Xiong, J.; Thangavel, G.; Wang, J.; Zhou, X.; Lee, P.S. Self-healable sticky porous elastomer for gas-solid interacted power generation. *Sci. Adv.* **2020**, *6*, eabb4246. [[CrossRef](#)]
21. Huang, L.; Lin, S.; Xu, Z.; Zhou, H.; Duan, J.; Hu, B.; Zhou, J. Fiber-Based Energy Conversion Devices for Human-Body Energy Harvesting. *Adv. Mater.* **2020**, *32*, e1902034. [[CrossRef](#)] [[PubMed](#)]
22. Han, K.; Tang, W.; Chen, J.; Luo, J.; Xu, L.; Wang, Z.L. Effects of Environmental Atmosphere on the Performance of Contact-Separation Mode TENG. *Adv. Mater. Technol.* **2018**, *4*, 1800569. [[CrossRef](#)]
23. Chen, J.; Tang, W.; Lu, C.; Xu, L.; Yang, Z.; Chen, B.; Jiang, T.; Wang, Z.L. Characteristics of Triboelectrification on Dielectric Surfaces Contacted with a Liquid Metal in Different Gases. *Appl. Phys. Lett.* **2017**, *110*, 201603. [[CrossRef](#)]
24. Lin, S.; Xu, L.; Tang, W.; Chen, X.; Wang, Z.L. Electron Transfer in Nano-Scale Contact Electrification: Atmosphere Effect on the Surface States of Dielectrics. *Nano Energy* **2019**, *65*, 103956. [[CrossRef](#)]

-
25. Sun, L.L.; Lin, S.Q.; Tang, W.; Chen, X.; Wang, Z.L. Effect of Redox Atmosphere on Contact Electrification of Polymers. *ACS Nano* **2020**, *14*, 17354–17364. [[CrossRef](#)] [[PubMed](#)]
 26. Schella, A.; Herminghaus, S.; Schröter, M. Influence of humidity on the tribo-electric charging and segregation in shaken granular media. *Soft Matter* **2017**, *13*, 394–401. [[CrossRef](#)]

Disclaimer/Publisher’s Note: The statements, opinions and data contained in all publications are solely those of the individual author(s) and contributor(s) and not of MDPI and/or the editor(s). MDPI and/or the editor(s) disclaim responsibility for any injury to people or property resulting from any ideas, methods, instructions or products referred to in the content.